



# High temperature oxidation kinetics of dysprosium particles



Brian J. Jaques, Darryl P. Butt\*

Department of Materials Science and Engineering, Boise State University, 1910 University Dr., Boise, ID 83725, USA  
Center for Advanced Energy Studies, 995 University Blvd., Idaho Falls, ID 83415, USA

## ARTICLE INFO

### Article history:

Received 28 January 2015  
Received in revised form 14 April 2015  
Accepted 25 April 2015  
Available online 1 May 2015

### Keywords:

Dysprosium  
Oxidation  
Kinetics  
Gas–solid reactions  
Rare earth alloys and compounds  
Corrosion

## ABSTRACT

Rare earth elements have been recognized as critical materials for the advancement of many strategic and green technologies. Recently, the United States Department of Energy has invested many millions of dollars to enhance, protect, and forecast their production and management. The work presented here attempts to clarify the limited and contradictory literature on the oxidation behavior of the rare earth metal, dysprosium. Dysprosium particles were isothermally oxidized from 500 to 1000 °C in N<sub>2</sub>–(2%, 20%, and 50%) O<sub>2</sub> and Ar–20% O<sub>2</sub> using simultaneous thermal analysis techniques. Two distinct oxidation regions were identified at each isothermal temperature in each oxidizing atmosphere. Initially, the oxidation kinetics are very fast until the reaction enters a slower, intermediate region of oxidation. The two regions are defined and the kinetics of each are assessed to show an apparent activation energy of 8–25 kJ/mol in the initial region and 80–95 kJ/mol in the intermediate oxidation reaction region. The effects of varying the oxygen partial pressure on the reaction rate constant are used to show that dysprosium oxide (Dy<sub>2</sub>O<sub>3</sub>) generally acts as a p-type semiconductor in both regions of oxidation (with an exception above 750 °C in the intermediate region).

Published by Elsevier B.V. This is an open access article under the CC BY-NC-ND license (<http://creativecommons.org/licenses/by-nc-nd/4.0/>).

## 1. Introduction

Global interest in rare earth element production and management has significantly increased in the past few years. In the year 2008, nearly \$190 million worth of rare earth materials were imported and used in the U.S. alone. Such “strategic materials” are sought after for use in metallurgical applications and alloys, electronics, catalysts, and cathode ray tubes [1]. Compared to the light rare earth metals, relatively little published literature exists for praseodymium, promethium, thulium, lutetium, and dysprosium (also known as the heavy rare earths) although scientific interest in these metals is on the rise. In the next forty years, Hoenderdaal et al. [2] project that the demand for dysprosia (Dy<sub>2</sub>O<sub>3</sub>) and other dysprosium compounds will increase to between 7 and 25 times (to 14–50 ktons) from the 2010 demand. Modern studies suggest that dysprosium is more abundant than 44 other elements in the earth’s crust (5.2 mg/kg) contrary to earlier perception, making its utility more available for emerging materials technologies [3].

According to Hoenderdaal et al. [2], the proposed increase in demand is due to the future of magnetic applications (electric

motors) due to dysprosium’s exceptional magnetic moment of 10.8 Bohr magnetons, which is second only to holmium [3], and its ability to induce coercivity as an alloying agent or dopant [3,4]. However, the demand for dysprosium has become more prevalent in other applications due to its many other interesting properties. For instance, dysprosium’s isotopes strongly absorb neutrons which lead to its use in nuclear reactor control rod moderator materials [3,5–7] and Dy<sub>2</sub>O<sub>3</sub> has been considered as a substitute for SiO<sub>2</sub> in high-k dielectric applications due to its large band gap (4.9 eV) and dielectric constant (14) [8,9]. Additionally, dysprosium mononitride (DyN) has been postulated as a suitable surrogate for americium mononitride (AmN) due to its similar physical and chemical attributes in studying its sintering and alloying effects in spent nuclear fuel reprocessing [10–15]. DyN has also been investigated as a material for ferromagnetic and semiconductor superlattice structures for spintronic applications [16–18].

Although a few manuscripts and reports were published in the late 1950s and 1960s on the oxidation behavior of dysprosium [19–22], the experiments were performed on monolithic samples (rather than powders or particles) and the results appeared to be contradictory. Of particular interest in this study is the high temperature oxidation kinetics of elemental dysprosium in the temperature range of 450–1000 °C in N<sub>2</sub>–(2%, 20%, and 50%) O<sub>2</sub> and Ar–20% O<sub>2</sub> using simultaneous thermal analysis techniques. An understanding of the oxidation kinetics of dysprosium has a wide

\* Corresponding author at: Boise State University, 1910 University Drive, Boise, ID 83725-2075, USA. Tel.: +1 208 426 1054.

E-mail address: [DarrylButt@BoiseState.edu](mailto:DarrylButt@BoiseState.edu) (D.P. Butt).

range of implications ranging from semiconductor and electronics applications, to “green” energy and electric motor (magnetic) applications, to nuclear power generation applications.

## 2. Experimental details

The starting material used to study the high temperature oxidation kinetics of dysprosium was dysprosium particles (99.7 wt% purity, ESPI) sieved through a 40 mesh (420  $\mu\text{m}$ ) sieve (Fig. 1). The particles had a surface area of  $0.20 \pm 0.06 \text{ m}^2 \text{ g}^{-1}$ , as determined by nitrogen adsorption Brunauer–Emmett–Teller (BET) techniques. The particles were characterized using X-ray diffraction (XRD) with a Cu K $\alpha$  source, as shown in Fig. 2. Additionally, minor concentrations of iron, yttrium, terbium, and tungsten (<3 ppm each) were identified in the starting material using a Thermo XSeries II quadrupole inductively coupled plasma mass spectrometry (ICPMS).

Oxidation experiments were performed using a high resolution simultaneous thermal analyzer (Netzsch STA 449) which is capable of collecting thermogravimetric analysis (TGA) and differential scanning calorimetry (DSC) data simultaneously. Approximately 30 mg of the dysprosium particles (sealed and stored in an argon filled glovebox) was loaded into an 85  $\mu\text{L}$  alumina combustion crucible which was immediately loaded in the STA furnace. In each case, a vacuum purge cycle was started using an oxygen-gettered ultra high purity (UHP) argon gas (<1 ppb oxygen). Once the chamber was fully purged, the thermal profile was started. The four process gases used for the oxidation studies presented in this manuscript were certified mixtures of N<sub>2</sub>–(2%, 20%, and 50%) O<sub>2</sub> and Ar–20% O<sub>2</sub>.

Non-isothermal oxidation data were first collected to determine suitable parameters to study the isothermal oxidation behavior. In the non-isothermal experiments, the furnace was ramped from 25 to 1100 °C at 20 °C/min in a gas flow rate of 100 mL/min while TGA and DSC data were collected. Each data set was replicated at least twice and the results were averaged. Isothermal oxidation experiments were completed in each of the atmospheres from 500 to 1000 °C. In each case, the temperature of the furnace was allowed to equilibrate for 5 min at the desired temperature prior to introducing the oxidizing atmosphere and the dysprosium particles were oxidized to completion. Each isothermal oxidation experiment was repeated 3–4 times. The isothermal oxidation data were averaged together and then the average mass gain was normalized by subtracting the initial mass gain (which was less than 0.1% in all cases). To account for geometry, the data was then divided by the maximum mass obtained and then multiplied through by the specific surface area (where the specific surface area is equal to the initial mass multiplied by the surface area of the particles obtained from B.E.T., as described above). This allowed for a direct comparison of data and accurate kinetics analysis using the specific mass gain with units of  $\mu\text{g}/\text{cm}^2$ .

## 3. Results and discussion

Dysprosium is reported to have a hexagonal close packed (HCP) crystal structure and a melting temperature of 1412 °C [3], although there also exists two other allotropes; a low temperature (<–187 °C) orthorhombic phase (Cmcm) and a high temperature (>1381 °C) face centered cubic (FCC) phase (Im $\bar{3}$ m) [3]. As seen in Fig. 2, the starting material for the oxidation studies presented here is primarily a HCP dysprosium phase (P63/mmc) with a small fraction of the high temperature FCC phase. The HCP and FCC cubic phases were identified using X-ray diffraction data from the International Centre for Diffraction Data (ICDD) database provided by Spedding et al. [23] and Curzon et al. [24], respectively. Additionally, it is important to note that the diffraction peaks were slightly shifted from the reported positions (depicted by the diamonds and circles in Fig. 2), which is discussed in more detail later in this manuscript. Although the authors understand that the geometry and morphology of the particles are not ideal for an oxidation kinetics study, the authors were unable to identify a vendor to provide single phase dysprosium particles (with minimal oxide). However, the dysprosium particles from ESPI were nearly single phase and had a low surface area which reduced un-wanted oxidation during handling.

Fig. 2 also shows a typical diffraction pattern obtained from a fully oxidized dysprosium sample in each of the atmospheres and temperatures investigated. The particular diffraction pattern shown is the result of oxidizing the dysprosium particles completely in N<sub>2</sub>–20% O<sub>2</sub> at 800 °C, which formed a cubic Dy<sub>2</sub>O<sub>3</sub> phase (Ia $\bar{3}$ ), as compared to data in the ICDD database provided by Swanson et al. [25]. Additionally, as shown by the inverted triangles, the oxide diffraction peaks agree well with the published values for Dy<sub>2</sub>O<sub>3</sub>. It is also worth pointing out that there are peaks in all of the oxide diffraction patterns that were not able to be indexed, as shown in Fig. 2.

TGA and DSC data were simultaneously collected during non-isothermal oxidation of dysprosium particles in each of the

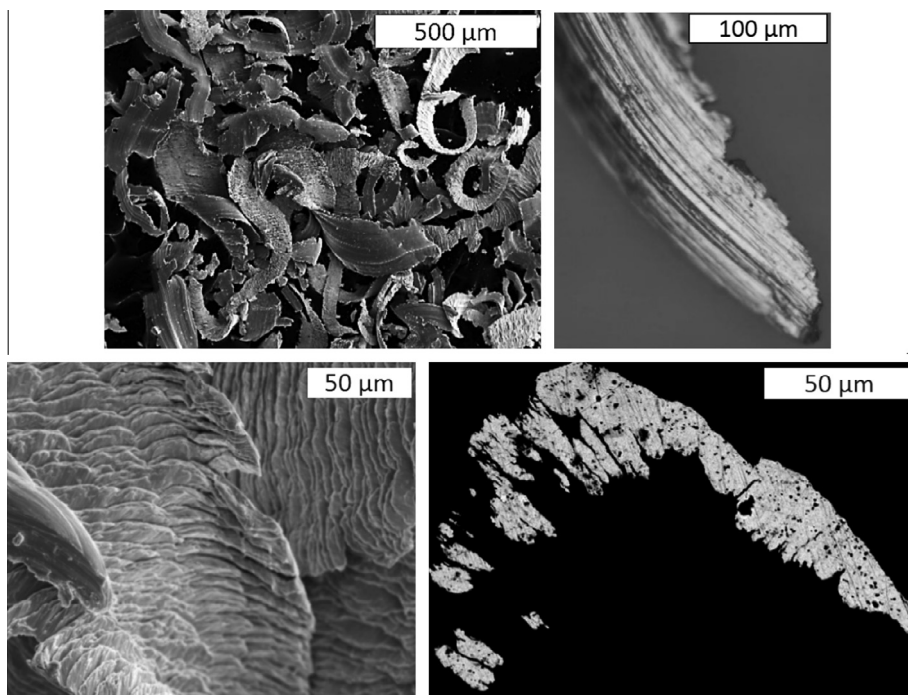


Fig. 1. Images of the dysprosium particles used as the starting materials for the high temperature oxidation reaction study. The particles have a surface area of  $0.20 \pm 0.06 \text{ m}^2 \text{ g}^{-1}$  as determined via gas adsorption techniques.

Download English Version:

<https://daneshyari.com/en/article/7998371>

Download Persian Version:

<https://daneshyari.com/article/7998371>

[Daneshyari.com](https://daneshyari.com)